Light Metals 2014
Edited by: John Grandfield
TMS (The Minerals, Metals & Materials Society), 2014

HIGH TEMPERATURE COMPRESSION TEST TO DETERMINE THE ANODE PASTE MECHANICAL PROPERTIES

Stéphane Thibodeau[1], Hicham Chaouki[1], Houshang Alamdari[1,2], Donald Ziegler[3], Mario Fafard[1*]
[1]NSERC/Alcoa Industrial Research Chair MACE[3] and Aluminium Research Centre−REGAL,
Laval University, Québec, QC, G1V0A6, Canada
[2]Department of Mining, Metallurgical and Materials Engineering, 1065 avenue de la Médecine
Laval University, Quebec, QC, G1V0A6, Canada
[3]Alcoa Primary Metals, Alcoa Technical Center, 100 Technical Drive Alcoa Center, PA 15069-0001, USA

Keywords: Axial and tangential strain, Carbon paste, Compression test, Flexible mould, Mechanical properties, Tomography.

Abstract

In order to develop a constitutive law for Hall process anode finite element modelling, a compression test method was developed to identify the hot paste properties which evolve with the density. A thin stainless steel cylindrical mould was placed in a furnace mounted on a press. The mould was instrumented with strain gages in the axial and tangential directions to capture the strain as a function of the axial load applied on the paste. The compression test meets the need for characterizing the paste mechanical properties. Loadings were designed to excite the specific mechanical properties, as a function of density, useful for the numerical model. The deformation of the mould shell allowed evaluation of the paste Young's modulus. A compaction test was performed and a tomography scan was realized on the resulting sample to confirm that the green compact density is almost uniform.

Introduction

The aluminium smelting industry consumes a large quantity of carbon anodes. Their production is an important part of the aluminium manufacturing process and good quality anode helps reduce both the carbon and smelting energy consumptions.

To form green anodes in a mould, one can use either pressing using a high-pressure load or a vibrocompaction process with significantly lower load. The temperature of the paste is kept near 150 °C during the forming process. During compaction, stress gradients through the paste induce considerable density gradients in the green anode blocks. The density gradient, in turn, affects the anode properties resulting in inhomogeneous electrical conductivity, chemical reactivity, and mechanical properties.

Numerical simulation of the forming process is a powerful tool to improve the anode forming process and thus, anode quality. Chaouki *et al.* [1] have simulated the pressing of the green carbon paste according to a macroscopic model capable of predicting the mechanical behaviour of the paste. Considering the paste as a nonlinear compressible viscoplastic gave good results in predicting the anode compaction behaviour.

The aim of this paper lies in the design of a characterization method of the mechanical properties of the hot carbon paste able to identify a three-dimensional constitutive law. A method using a thin wall deformable mould has been developed to characterize the paste Young's modulus, Poisson's ratio and the time dependency.

Materials and Methods

The carbon paste elaboration

The paste recipe used in the compression tests was designed based on one currently used by the industry [2, 3]. The paste is constituted of calcined petroleum coke and coal tar pitch. The calcined coke is included in the recipe under two forms: large aggregates and fine particles. The latter are produced by ball milling of calcined coke until a Blaine number of 4200 is reached. Table 1 summarizes the details of the recipe [2, 3]. The dry percentage corresponds to the aggregates and fines and excludes the coal tar pitch. The mix percentage considers the fraction of all the constituents of the paste.

Table 1: Recipe of the paste used during the compression tests.

Aggregate sizes (US Mesh)	**Mass** (g)	**% dry**	**% mix**
-4 +8	1072.6	21.8	17.9
-8 +14	487.1	9.9	8.1
-14 +28	565.8	11.5	9.4
-28 +48	619.9	12.6	10.3
-48 +100	447.7	9.1	7.5
-100 +200	521.5	10.6	8.7
Fines	1205.4	24.5	20.1
Pitch	1080.0	-	18.0
Total	6000.0	100	100

The ingredients are mixed together following a specific sequence in order to obtain the carbon paste. The aggregates and fines were first preheated for 120 minutes to eliminate the moisture. Coal tar pitch was then added to the hot coke particles and heated for another 30 minutes. Finally, all the raw materials were mixed during 10 minutes to homogenize the mixture. The mixer was installed in a furnace in order to maintain the paste temperature at 178°C while mixing [2, 3]. The mixing time and temperature have been chosen in order to obtain the maximum paste density [3].

Experimental setup

Mechanical properties of the paste were characterized based on a compaction test in the flexible mould. The compression tests were performed using a DARTEC hydraulic press with a motionless crosshead, a piston underneath that generates the load and a load cell with a maximum capacity of 250 kN (Fig. 1). In order to uniformly apply the load on the entire surface of the paste, 30 mm thick steel plates are fixed to the lower and upper pistons. The upper plate is machined with a diameter slightly smaller than the inner diameter of the mould. During the compression test, this plate ends up inside the mould. A groove is machined on its side to allow introducing a thermocouple into the middle of the paste.

The mould, constituted of 3 pieces, is placed between the piston plates (Fig. 1). A 6 mm steel plate is used as the base of the mould. To avoid any displacement in the directions perpendicular to the axis, a rabbet is machined to receive the mould shell. A 25 mm thick aluminium spacer, having the same diameter as the upper plate, is used as the top of the mould. The spacer has a tapped hole in the middle of the top face to facilitate the manipulations. Grooves are machined on the top and the thermocouple is introduced into the paste passing through these grooves then a small hole drilled across the thickness. A thin stainless steel shell having a cylindrical shape is the most important part of the mould. The mould is free of joints, and has a uniform thickness of 0.356 mm. The mould wall diameter and height are respectively 254 mm and 140 mm. During the compression test, the paste is squeezed between the piston plates and exerts a radial force on the shell.

The shell of the mould has been selected with dimensions that allow its elastic deformation when subjected to the loads it experiences during the pressing tests. The elastic properties of the thin wall shell have been measured in the laboratory: E_s = 220 GPa and ν_s = 0.31. The shell is instrumented with 8 high temperature strain gages; 4 strain gages are placed in the axial direction and 4 in the tangential direction. The strain gages are placed by pair (axial and tangential) at 90° from each other. The large diameter and the thinness of the mould help to give rise to significant deformations.

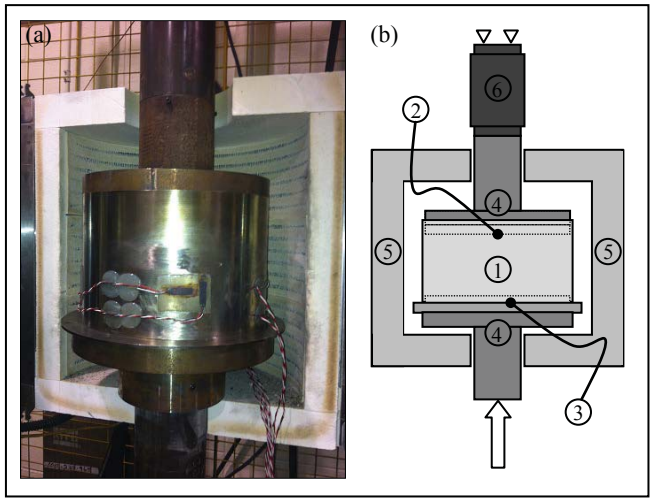

Fig. 1: (a) Photograph and (b) Schematic representation of the apparatus (1. Mould, 2. Spacer with insert, 3. Bottom plate, 4. Piston with plates fixed, 5. Furnace, 6. Load cell).

The mould was inserted in a furnace used to maintain the temperature at 150 °C during the compression test. The oven was used to preheat the mould at 165 °C. Fifteen degrees of superheat were required to compensate the temperature loss that occurs during mould filling.

Assembling and test procedures

In order to perform the compression tests on a fresh carbon paste that has not undergone large temperature variations, a sequence of manipulations must be executed in a minimal amount of time. Beforehand, the oven mounted on the press preheats the mould during the same period used to prepare the paste. Once the procedure to prepare the paste is completed, a thin film of lubricant, made of 13 mass percent "mobilcut 102" oil in water, is sprayed on the inside of the mould. The paste is then poured into the mould shell mounted on the rabbet of the base plate. The spacer is carefully inserted inside the mould shell. The thermocouple is placed in the paste through the small hole in the spacer. The mould is replaced in the oven and the piston of the press is slowly moved up to manually align the top piston plate inside the mould until the distance between the upper end lower plates reaches 137 mm. The oven is then closed.

The compression test is started once the paste temperature is stabilized at 150±1 °C. For a simple compression test, the bottom piston has a constant upwards velocity of 1 mm/s until the axial force reaches 225 kN. The displacement is then reversed to its initial position in order to release the mould.

Characterization of the paste mechanical properties

In the first part of this work, the characterization of the paste Young's modulus and Poisson's ratio requires evaluating the stress and strain states of the paste. Hypotheses, based on the applied axial load on the paste and both axial and tangential mould strains, are formulated in order to evaluate the unknown stresses and strains of the paste (σ_{rr_p}, $\sigma_{\theta\theta\_p}$, σ_{zz_p}, ε_{rr_p}, $\varepsilon_{\theta\theta\_p}$, ε_{zz_p}). The axial load is obtained from the load cell of the press and the axial and tangential strains are measured with the strain gages. Within the following development, the mould strains are defined as the average of the measured strains recorded by four strain gages. The subscript *"p"* refers to the paste and *"s"* to the steel of the mould shell.

Within the cylindrical mould, the radial stress generated by the paste (σ_{rr_p}) corresponds to the mould shell reaction in the radial direction. Eq.1 and eq.2 define the tangential stress within the mould wall. The first equation is based on the mechanical properties of the mould steel and the measured strains. The second equation is based on the theory of the hollow cylinder subjected to internal pressure (P_i), therefore to the desired radial stress (σ_{rr_p}).

$$\sigma_{\theta\theta\_s} = \frac{E_s}{(1+\nu_s)(1-2\nu_s)}\left[(1-\nu_s)\varepsilon_{\theta\theta\_s} + \nu_s\left(\varepsilon_{rr\_p} + \varepsilon_{zz\_p}\right)\right] \quad (1)$$

$$\sigma_{\theta\theta\_s} = \frac{a^2P_i - b^2P_o}{b^2 - a^2} + \frac{(P_i - P_o)a^2b^2}{r^2(b^2-a^2)} \quad (2)$$

where a and b are the inner and outer radius of the mould shell and r is the evaluated position of the tangential stress in the radius direction. In eq.1, the mould radial strain is negligible due to the thinness of the shell and in eq.2 external pressure is nil. Eq.2 is evaluated at the interface paste-mould ($r = a$). Solution of eq.1 and eq.2 provides the relation of the radial stress to the measured mould strains.

$$\sigma_{rr\_p} = P_i = \frac{b^2 - a^2}{b^2 + a^2}\frac{E_s}{(1+\nu_s)(1-2\nu_s)}\left[(1-\nu_s)\varepsilon_{\theta\theta\_s} + \nu_s \cdot \varepsilon_{zz\_s}\right] \quad (3)$$

The paste and mould tangential deformations are assumed to be equal because the mould radial strain has been neglected. These tangential deformations are respectively defined as the eq.4 and eq.5 using axisymmetric hypothesis:

$$\varepsilon_{\theta\theta\_p}\big|_{r=a} = \frac{u_a}{a} \quad (4)$$

$$\varepsilon_{\theta\theta\_s}\big|_{r=b} = \frac{u_b}{b} \quad (5)$$

Eq.6 shows that the variation of the paste radius is equivalent to the variation of the external wall ($r = b$) plus the radial deformation of the wall that was neglected. Because the shell thickness-to-radius ratio is very small, the paste tangential strain becomes almost equal to the mould tangential strain:

$$\varepsilon_{\theta\theta\_p} = \frac{u_a}{a} = \frac{u_b + \varepsilon_{rr\_s}}{a} \cong \frac{u_b}{a} \cong \frac{u_b}{b} = \varepsilon_{\theta\theta\_s} \quad (6)$$

At $r = 0$, $u = 0$ and at b, $u = u_{max}$ where $\varepsilon_{\theta\theta\_s}$ is measured.

One may demonstrate that the paste undergoes the same strain in both tangential and radial directions. Per definition, the radial strain is the change in length per unit length in the radial direction, which is constant over the whole radius (axisymmetric geometry). When the radial strain is evaluated at the maximal radius ($r=a$), and using eq. 6, it becomes easy to agree that the paste radial and tangential strains are equivalent:

$$\varepsilon_{rr\_p} = \left.\frac{\partial u_r}{\partial r}\right|_{r=a} = \frac{u_a}{a} = \varepsilon_{\theta\theta\_p} \quad (7)$$

The next hypothesis is based on the equilibrium equations in cylindrical coordinates [4]:

$$\varepsilon_{rr\_p} = \frac{1}{E_p}\left[\sigma_{rr\_p} - \upsilon_p\left(\sigma_{zz\_p} + \sigma_{\theta\theta\_p}\right)\right] \quad (8)$$

$$\varepsilon_{\theta\theta\_p} = \frac{1}{E_p}\left[\sigma_{\theta\theta\_p} - \upsilon_p\left(\sigma_{rr\_p} + \sigma_{zz\_p}\right)\right] \quad (9)$$

$$\varepsilon_{zz\_p} = \frac{1}{E_p}\left[\sigma_{zz\_p} - \upsilon_p\left(\sigma_{\theta\theta\_p} + \sigma_{rr\_p}\right)\right] \quad (10)$$

Using result (7), it is easy to demonstrate that, for a pure bi-axial loading, the paste radial stress is equal to the tangential one. Thus, eq.8 is equal to the eq.9 ($\varepsilon_{rr\_p} = \varepsilon_{\theta\theta\_p}$):

$$\frac{1}{E_p}\left[\sigma_{rr\_p} - \upsilon_p\left(\sigma_{zz\_p} + \sigma_{\theta\theta\_p}\right)\right] = \frac{1}{E_p}\left[\sigma_{\theta\theta\_p} - \upsilon_p\left(\sigma_{rr\_p} + \sigma_{zz\_p}\right)\right] \quad (11)$$

By simplifying the previous equality one can write:

$$\sigma_{rr\_p}\left(1 + \upsilon_p\right) = \sigma_{\theta\theta\_p}\left(1 + \upsilon_p\right) \quad (12)$$

Thus, the equality between the radial and tangential stress is proven.

The paste axial strain is evaluated as properly defined:

$$\varepsilon_{zz\_p} = ln\left(\frac{h}{h_0}\right) \quad (13)$$

where the height (h) is measured from the LVDT of the press.

The applied axial stress on the paste is reduced due to the friction at the interface mould-paste. The normal force to the mould wall (σ_{rr_p}) is assumed to be uniform all over the mould-paste interface.

$$F_p = F_{applied} - F_f \quad (14)$$

Using the Coulomb friction model, F_f is defined as the friction coefficient multiplied by the normal applied force [5].

$$F_f = \mu \cdot \sigma_{rr\_p} \cdot 2\,\pi\, a\, h_p \quad (15)$$

where the paste height is obtained using the LVDT of the press during the compression test. The applied axial stress on the paste becomes:

$$\sigma_{zz\_p} = \frac{F_p}{\pi a^2} = \frac{1}{\pi a^2}\left[F_{applied} - \mu \cdot \sigma_{rr\_p} \cdot 2\,\pi\, a\, h_p\right] \quad (16)$$

Based on eq.9 and eq.10, the Young's modulus and the Poisson's ratio of the paste can be defined as a function of known variables. All required stresses and strains are function of the measured axial and tangential strains of the mould shell and may be obtained using the previous hypotheses. The solution for the Young's modulus and Poisson's ratio has been obtained using Maple software (eq.17 and eq.18):

$$E_p = \frac{2\sigma_{\theta\theta\_p}^2 - \sigma_{\theta\theta\_p} \cdot \sigma_{zz\_p} - \sigma_{zz\_p}^2}{2\varepsilon_{\theta\theta\_p} \cdot \sigma_{\theta\theta\_p} - \varepsilon_{zz\_p} \cdot \sigma_{zz\_p} - \varepsilon_{zz\_p} \cdot \sigma_{\theta\theta\_p}} \quad (17)$$

$$\upsilon_p = \frac{\varepsilon_{\theta\theta\_p} \cdot \sigma_{zz\_p} - \varepsilon_{zz\_p} \cdot \sigma_{\theta\theta\_p}}{2\varepsilon_{\theta\theta\_p} \cdot \sigma_{\theta\theta\_p} - \varepsilon_{zz\_p} \cdot \sigma_{zz\_p} - \varepsilon_{zz\_p} \cdot \sigma_{\theta\theta\_p}} \quad (18)$$

In order to characterize the Young's modulus and Poisson's ratio as a function of the paste density, a compression test was designed to capture the elastic perturbation at different levels of compaction. A repeated pattern allows capturing the elastic behaviour relative to different densities ranging from 800 to 1600 kg/m^3. Fig.2 shows the imposed loading for this characterization. The test is controlled in displacement. The paste height is linearly reduced by 3 mm then released by 1 mm. This pattern is repeated until the applied axial force reaches 225 kN. The small perturbations of the paste mechanical behaviour are captured through the strains induced on the steel shell by means of the strain gages. Note that it is important to calculate the Young's modulus and Poisson's ratio from the small perturbations illustrated by the pairs of points (Fig.2 – magnification) and not from the deformation relative to the initial height of the paste. The elastic properties can be estimated according to both loading and unloading perturbations.

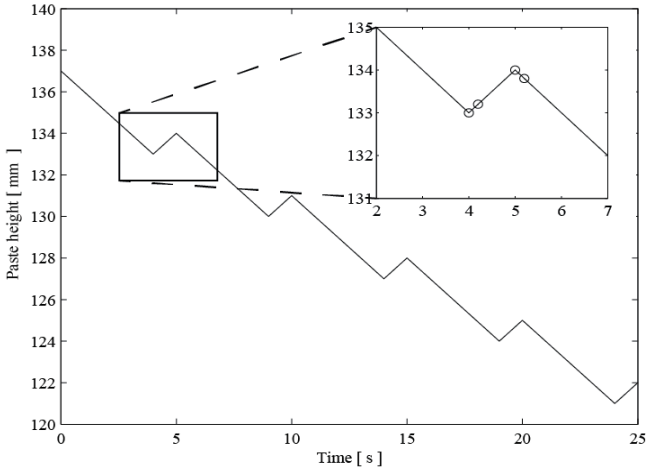

Fig. 2: Typical displacement command to determine the elastic properties of the paste as a function of the paste density.

In the second part of this work, the paste viscosity was characterized assuming that the paste has viscoplastic behaviour. Fig.3 presents the Maxwell viscoplastic rheological model used for this characterization. Within this model, the total strain is the summation of the elastic (ε^e) and viscous (ε^v) strains.

Fig. 3: Viscoplastic rheological model: spring and dashpot in series.

The general solution corresponding to a Maxwell model under a constant strain can be easily obtained:

$$\sigma_{zz\_p}(t) = \eta\dot{\varepsilon} + (\sigma_0 - \eta\dot{\varepsilon})e^{-\frac{E}{\eta}t} \quad (19)$$

To characterize the paste viscosity as a function of the paste density, the compression test was designed as a series of relaxation tests covering the densities ranging from 800 to 1600 kg/m^3. The paste height is reduced by 1 mm and maintained during 10 s for each of these steps. Fig.4 presents the imposed displacement (solid line) and a typical paste axial stress (dashed line) associated to each of these steps. The test was performed until the axial force reached 225 kN.

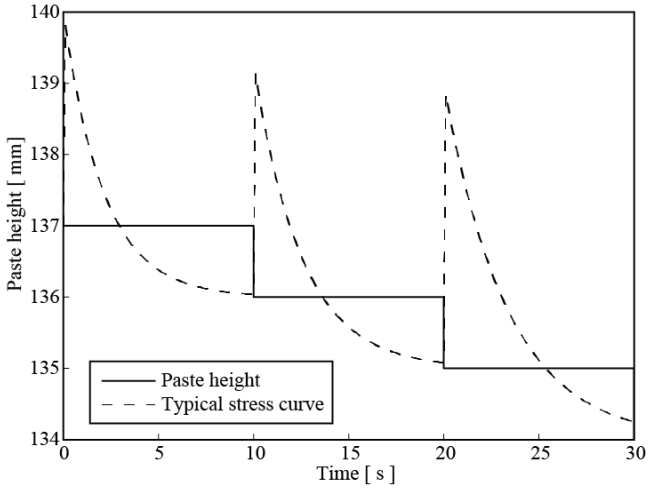

Fig. 4: Typical displacement command and axial stress to determine the paste viscosity as a function of the density.

Within this test, every step needs to be considered and evaluated as a distinct test. The variation of the total strain becomes ($\dot{\varepsilon}$) nil and eq.19 becomes:

$$\sigma_{zz\_p}(t) = \sigma_0 e^{-\frac{E}{\eta}t} \quad (20)$$

The treatment of the results obtained by this test requires the Young's modulus function obtained with the first test. The axial stress is recorded by the load cell, thus the initial axial stress (σ_0) is known for each step. According to the levels of compaction, the paste viscosity behaviour can be evaluated, using curve fitting, as a function of the density ($\eta(\rho)$).

Results and discussion

Young's modulus and Poisson's ratio compression test

The test, designed to characterize the paste Young's modulus and Poisson's ratio, has produced reasonable shell deformation to measure the strains. These perturbations have permitted evaluation of all the stress and strain states of the paste. Fig. 5 presents the relative axial and tangential stresses and strains of the paste in function of time for an entire test (values divided by the absolute maximum value).

The axial and tangential stresses undergo a severe increase after 75 s of the test (Fig. 5a and c). Thibodeau *et al.* [2] demonstrated that when the paste reaches a certain level of compaction, the rigid skeleton is formed, and then the axial force must be drastically increased to generate additional deformation. For the same reason, the Poisson's ratio effect becomes important at the same instant. Before this compaction level, the axial applied force is mostly dissipated by the permanent paste deformation. After this point, a part of the force is transmitted to the perpendicular direction through the rigid skeleton causing the tangential and radial strains. Fig. 5b presents the paste axial strain. Since this curve is based on specified displacement, no slope or other change is observed when the skeleton is established.

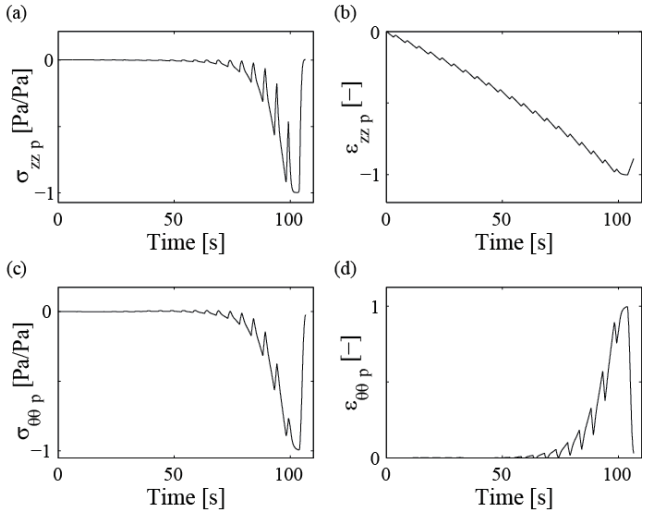

Fig. 5: Curves presenting the relative value of (a) σ_{zz_p}, (b) ε_{zz_p}, (c) $\sigma_{\theta\theta\_p}$ and $\varepsilon_{\theta\theta\_p}$ as functions of time during an entire loading test.

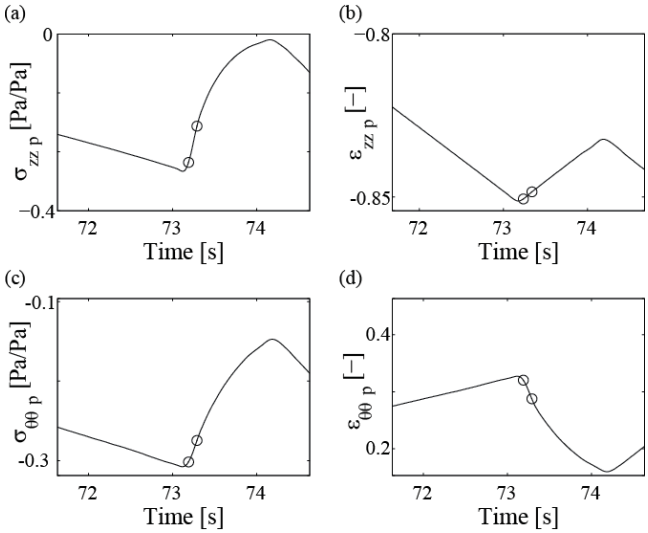

Fig. 6: Curves presenting the relative value of (a) σ_{zz_p}, (b) ε_{zz_p}, (c) $\sigma_{\theta\theta\_p}$ and $\varepsilon_{\theta\theta\_p}$ in function of the time according to a local unloading.

Based on this explanation, one may understand that the Young's modulus and the Poisson's ratio are evolving with the paste density. To properly characterize these paste parameters as a function of the paste density, eq.17 and eq.18 need to be evaluated at different levels of compaction. The entire test is segmented so that each loading/unloading cycle becomes a test in itself. Fig. 6 presents a magnification of a typical unloading segment extracted from the Fig. 5. The involved stresses and strains in these equations are the difference between the points illustrated on each

graph. The differences need to be taken from a linear instantaneous behaviour to avoid capturing the time dependency behaviour.

Fig. 7 presents the paste relative Young's modulus as a function of paste density as obtained experimentally. The Young's modulus used in the simulation performed by Chaouki *et al.* [1] is added in the aim of comparison. The Young's modulus evaluated according to the loading elastic part of the curves is undervalued comparatively to the one from the unloading parts. This is due to the fact that the load has not been entirely removed between each step, thus a "creep" deformation is added to the instantaneous elastic deformation. However, the two evaluated Young moduli follow a similar tendency with a relatively low value for a paste density less than 1300 kg/m^3. The value considerably increases beyond this point [2]. The Young modulus employed by Chaouki *et al.* [1] in the simulation is lower than those obtained from the characterisation method. It has been calculated from eq.21 where μ and λ (eq.22 and eq.23) are the Lamé coefficients used in the model. The calculated Young modulus is situated in a reasonable range and has a very similar shape to the two others. Chaouki *et al.* have obtained an excellent mechanical behaviour prediction of the paste using a good combination of mechanical properties. However, the slight difference between the Young modulus from the inverse method and those obtained from the experiment might be explain by an overvaluation of other parameters belonging of this combination. Thus, the error may be hidden within this combination.

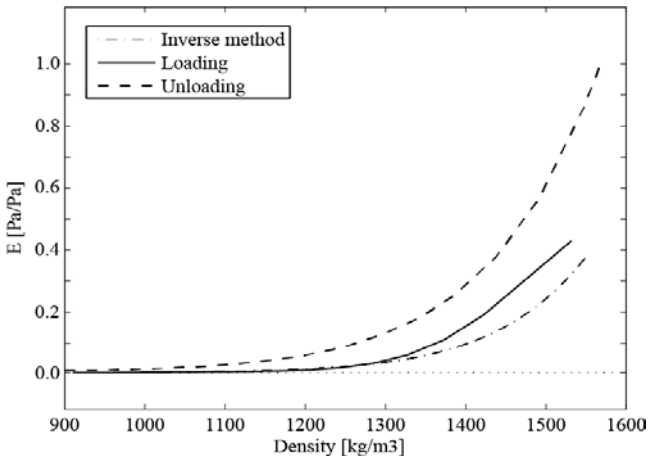

Fig. 7: Paste relative Young's modulus as a function of the paste density obtained from the experimental method. From [1].

$$E = \frac{\mu(III_G) \cdot \left(3\lambda(III_G) + 2\mu(III_G)\right)}{\lambda(III_G) + \mu(III_G)} \quad (21)$$

The parameters from Chaouki *et al.* used to define the Young modulus (with $III_G = \rho_0/\rho$):

$$\mu(III_G) = \hat{\mu} \cdot (1 + \lambda_1(\rho_0/\rho)^{-2n_1})^{q_1} \quad (22)$$

$$\lambda(III_G) = \alpha \cdot exp\left(\frac{1 - (\rho_0/\rho)}{\beta}\right) \quad (23)$$

Time dependency compression test

The analyses of the time dependency behaviour are currently in progress. Nonetheless, the experiment has been performed. The Fig. 8 presents the imposed displacement and the relative axial stress response for a whole test. As for the preceding characterization, each step of this test is considered as a single creep test using a constant paste height.

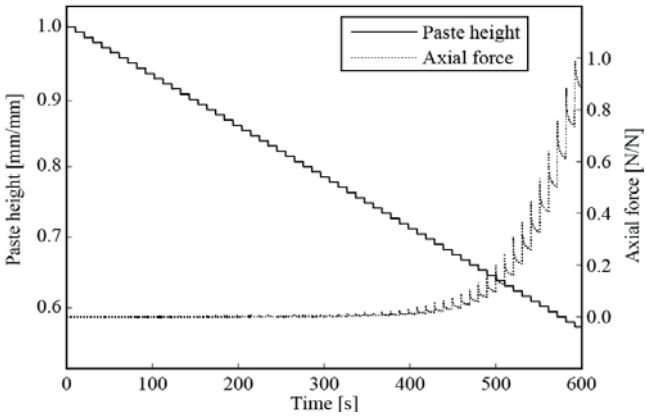

Fig. 8: Curves presenting the relative paste height and the resulting relative axial force in function of the time.

Fig. 9 shows the higher magnification of the Fig. 8 for the time ranging from 400 to 450 s. The stress curves (dash line) seem to follow an exponential behaviour that corresponds to the obtained solution (eq.20). Using a curve fitting and the Young's modulus corresponding to the appropriate paste density, the time dependency parameter (η) becomes easily evaluable.

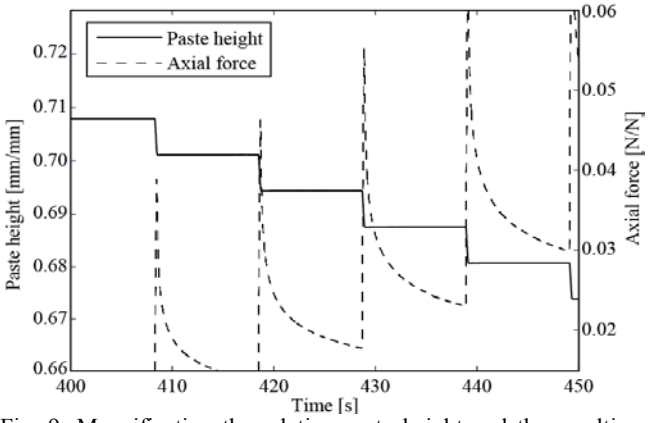

Fig. 9: Magnification the relative paste height and the resulting relative axial force in function of the time.

In light of the experimental results related to the two tests, the methodology developed in the aim to determine the carbon paste properties (E, ν and η) as a function of the paste density appears hopeful. However, the Young's modulus of the paste needs to be accurately evaluated from an appropriate test to correctly characterize the time dependency behaviour.

Green compact and computerized tomography (CT-scan)

Fig. 10 shows a green sample compacted in the laboratory; the mechanical behaviour of this test has been simulated by Chaouki *et al.* [1]. The paste has been pressed at 150 °C using the apparatus described above. A linear displacement was applied to the paste until the applied pressure reached 4.5 MPa. The load was removed, and then the green compact was removed before freezing of the pitch. The compact has a height of approximately 76 mm giving a density of 1550 kg/m^3 (Fig. 10).

Fig. 10: Photography of the green compact, pressed in laboratory.

X-ray tomography scanning was performed on the resulting sample using a medical scanner (Somatom Sensation 64 at INRS-ETE research centre in Quebec City) [6]. Image processing allowed the estimation of the density gradient through a colour map. Fig. 11 shows a relative density mapping according to CT numbers. These numbers need to be calibrated as a function of the material to express the apparent density.

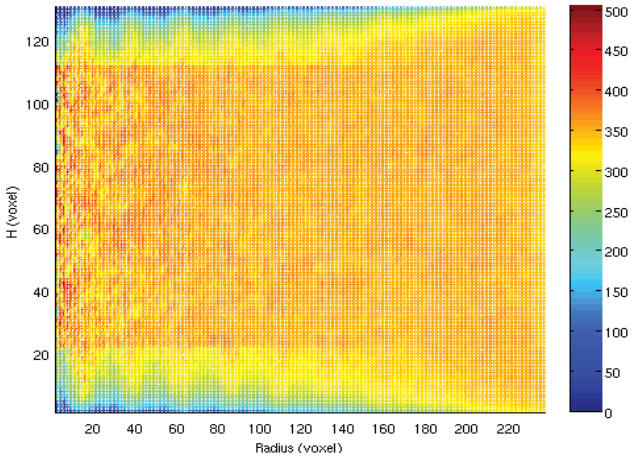

Fig. 11: Processed image of the tomography of the green compact presented as a function of the radius (red means high density and blue means low density).

In Fig. 11, the top and bottom of the figure show blue zones caused by the scanning method. Measurement artefacts due to the surrounding air create these zones. Along the H axis (radius = 0), the perturbation is introduced by an averaging over fewer points. Thus, the carbon compact does present only a very slight density gradient in the radial direction. However, the local variations in the density allow appreciating the CT scan as an excellent method for generating a mapping density of a carbon block.

Conclusions

Within this paper, a method to characterize the high temperature carbon paste mechanical properties as a function of the paste density has been presented. The developed compression test using a thin deformable shell seems to meet the needs of this characterization with its ability to deform without being damaged.

The Young's modulus as a function of the density has been satisfactory evaluated when compared to Chaouki *et al.* [1]. Loadings were designed to excite the specific mechanical properties as a function of density. The produced perturbations (Fig. 6) allowed evaluating all the stress and strain states of the paste required for this analysis. Their evaluations are based on the measured mould shell deformation, paste height (LVDT) and axial applied force (load cell).

The analysis of the time dependent behaviour is currently in progress. The viscoplastic model seems to be able to accurately predict the mechanical behaviour of the paste. The experimental stress curves (Fig. 9) show an exponential shape as expressed by the viscoplastic model solution. However, the characterization of the time dependent behaviour requires caution because it is strongly dependent on the Young's modulus, which needs to be accurately evaluated.

The tomography is revealed to be a good approach to obtain the density mapping of the green carbon sample. Image processing is necessary to appropriately appreciate variations within the density. Tomography scanning was performed on the resulting sample, of which the mechanical behaviour was simulated. Except scan and data treatment artefacts, no significant density gradient is present within this form of compact. A calibration is required according to this material in order to convert the CT number into the apparent density (see [6] for more details on the calibration). The mapping density becomes an appropriate base of comparison with the numerical simulation to validate the mechanical parameters obtained from the experimental method.

Acknowledgments

Authors would like to acknowledge the financial support of Natural Sciences and Engineering Research Council (NSERC) and Alcoa. A part of the research presented in this paper was financed by the Fonds de Recherche du Québec-Nature et technologies (FRQ-NT) by the intermediary of the Aluminium Research Centre-REGAL. Particular thankfulness is dedicated to Hugues Ferland, from the REGAL-LAVAL research centre for its help in the development of the apparatus and the execution of the tests in laboratory.

References

[1] H. Chaouki, S. Thibodeau, H. Alamdari, D. Ziegler and M. Fafard, "Viscoplastic Modeling of the Green Anode Forming Process," *Light Metals Proceeding, San Diego, CA, March 16-20,* TMS 2014.

[2] S. Thibodeau, H. Alamdari, D. Ziegler and M. Fafard, "New insight on the restructuring and breakage of particles during uniaxial confined compression tests on aggregates of petroleum coke," 2013 (Submited to Powder Technology - Ms. Ref. No.: POWTEC-D-13-01233).

[3] K. Azari, H. Alamdari, G. Aryanpour, D. Picard, M. Fafard and A. Adams, "Mixing variables for prebaked anodes used in aluminum production," *Powder Technology,* vol. 2235, pp. 341-348, 2013.

[4] E. Volterra and J. H. Gaines, Advanced Strenght of Materials, N. J.: Prentice Hall, 1971.

[5] S. Thibodeau, H. Alamdari, D. Ziegler and M. Fafard, "Tribological behaviour of the green anode paste with a steel plate at 150°C," *Wear,* (To be submitted - 2013).

[6] D. Picard, H. Alamdari, D. Ziegler, B. Dumas and M. Fafard, "Characterization of Pre-Backed Carbon Anode Samples Using X-Ray Computed Tomography and Porosity Estimation," *Light Metals Proceeding,* TMS 2012.